in this case, an optimum value of the parameter α can be determined self-consistently via the following iterative scheme:

(i) Assign an initial value to α in an arbitrary way.
(ii) Solve the matrix equation to obtain k_0^2 as an eigenvalue (note that β is given as an input datum).
(iii) Calculate α according to (6).
(iv) Iterate the above procedures (ii) and (iii) until the solution converges within required accuracy.

Although this method includes only one decay parameter, it does not require the calculation of the eigenvector.

III. Numerical Example

To demonstrate the power of the present algorithms, we consider a round optical fiber since its exact solution is readily available. Making use of symmetry nature, we divide only one quarter of the cross section into quadratic finite and infinite elements, as illustrated in Fig. 3. As a finite element scheme, we use the scalar formulation [2], [3].

Table I exhibits an example of the analyzed results, where the index difference $\Delta = 1$ percent, $n_{cl} = 1.46$, and $\beta a = 6$ (a: core radius), and the initial set of the parameters is $\alpha_x/\beta = \alpha_y/\beta = 0.1$. Note that $\beta a = 6$ corresponds to a case very near cutoff. It is readily found from the table that sufficiently accurate solutions are obtainable only with one time of iteration. On the other hand, the solution for the simple truncation, in which the boundaries $x = x_0$, $y = y_0$ are assumed to be perfect conducting walls and no infinite elements are added to them, is far less accurate than that for the present algorithms.

Fig. 4 displays an example of the field distributions in the cross section. In this figure the region $|X| \geq 7$, $|Y| \geq 7$ corresponds to that divided into infinite elements. It is seen from the figure that the interface between finite-element and infinite-element regions is smooth in spite of only one time of iteration.

IV. Conclusions

A self-consistent finite-element approach for the eigenmode analysis of unbounded waveguides has been proposed using decay-type infinite elements. Two algorithms have been described for the determination of the unknown decay parameters. Through the application to the eigenmode analysis of an optical fiber, the power of this approach has been successfully demonstrated.

Acknowledgment

The authors would like to express their gratitude to the late Prof. Michio Suzuki of Hokkaido University for his advice and encouragement during his lifetime.

References

[1] M. Ikeuchi, H Sawami, and H. Niki, "Analysis of open-type dielectric waveguides by the finite-element iterative method," *IEEE Trans. Microwave Theory Tech.*, vol. MTT-29, pp. 234–239, Mar. 1981
[2] N. Mabaya, P. E Lagasse, and P Vandenbulcke, "Finite element analysis of optical waveguides," *IEEE Trans. Microwave Theory Tech* , vol MTT-29, pp. 600–605, June 1981.
[3] K. Hayata, M. Koshiba, and M. Suzuki, "Lateral mode analysis of buried heterostructure diode lasers by the finite-element method," *IEEE J. Quantum Electron.*, vol. QE-22, pp. 781–788, June 1986.
[4] K Hayata, M. Eguchi, M. Koshiba, and M. Suzuki, "Vectorial wave analysis of side-tunnel type polarization-maintaining optical fibers by variational finite elements," *J. Lightwave Technol* , vol. LT-4, pp. 1090–1096, Aug. 1986
[5] K Oyamada and T. Okoshi, "Two-dimensional finite-element method calculation of propagation characteristics of axially nonsymmetrical optical fibers," *Radio Sci.*, vol. 17, pp. 109–116, Jan.–Feb. 1982.
[6] C. Yeh, K. Ha, S. B. Dong, and W. P. Brown, "Single-mode optical waveguides," *Appl. Opt.*, vol 18, pp 1490–1504, May 1979.
[7] B. M. A. Rahman and J B Davies, "Finite-element analysis of optical and microwave waveguide problems," *IEEE Trans. Microwave Theory Tech.*, vol. MTT-32, pp. 20–28, Jan 1984.
[8] K. S. Chiang, "Finite element method for cutoff frequencies of weakly guiding fibres of arbitrary cross-section," *Opt. Quantum Electron.*, vol 16, pp. 487–493, 1984.
[9] R. B. Wu and C. H. Chen, "A variational analysis of dielectric waveguides by the conformal mapping technique," *IEEE Trans. Microwave Theory Tech.*, vol. MTT-33, pp. 681–685, Aug 1985.
[10] P. Bettess, "Infinite elements," *Int. J. Numer. Meth. Engrg.*, vol 11, pp. 53–64, 1977.
[11] P. Bettess, "More on infinite elements," *Int. J. Numer. Meth Engrg.*, vol. 15, pp. 1613–1626, 1980.

Analysis of Coupled Microslab™ Lines

BRIAN YOUNG AND TATSUO ITOH, FELLOW, IEEE

Abstract—**Symmetrically coupled Microslab lines are analyzed with a mode-matching method to build design charts for the propagation constant and characteristic impedance. Results are provided for GaAs/alumina Microslab implementations.**

I. Introduction

Microslab is a novel low-loss quasi-planar waveguide intended for use at millimeter-wave frequencies [1]. The single-line implementation has been studied and the results appear in [2], where a design procedure is presented which minimizes conductor loss, and design charts are given for implementation on GaAs substrates. This paper extends that work by analyzing the symmetrical coupled-line Microslab configuration. Design charts are provided for GaAs/alumina implementations to complement the results in [2]. The design charts to complete the GaAs implementation for insulating layer dielectric constants of 8.2 and 11.5 are not included due to the lack of space.

II. Analysis

The analysis method used to build the design charts is the mode-matching method. The particular procedure is based on the one used in [2]. The method is outlined below to provide the additional details necessary for the coupled-line implementation.

The symmetrically coupled Microslab is shown in Fig. 1. The metallizations are perfectly conducting with zero thickness, and the dielectrics are lossless. A cover plate is added to the structure to discretize the eigenvalue spectrum [3]. Since the strips have equal widths, the structure can be divided along the plane of symmetry with a magnetic (electric) wall to eliminate the odd (even) modes. The divided structure is further subdivided into four regions as shown in Fig. 2 for modal expansion. Extra dielectrics are added to the left and right of the strip in regions 1 and 4 to facilitate checking the program.

Manuscript received June 25, 1987; revised September 19, 1987. This work was supported in part by a grant from Martin Marietta Laboratories.

The authors are with the Department of Electrical and Computer Engineering, University of Texas at Austin, Austin, TX 78712.

IEEE Log Number 8718361.

Microslab is a trademark of the Martin Marietta Corporation. Patent pending

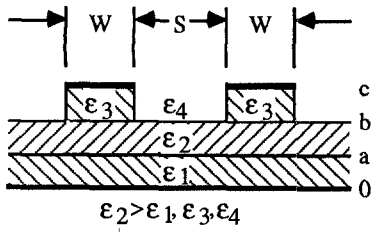

Fig. 1. Symmetric coupled-line Microslab.

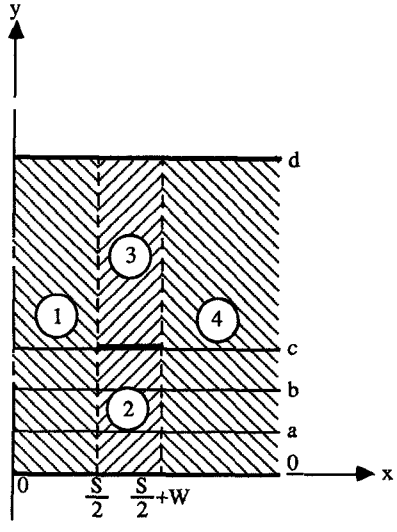

Fig. 2. Subdivision of Microslab into four regions for mode-matching analysis.

Each region is a section of layered parallel-plate waveguide. The fields in each are expanded in the parallel-plate waveguide modes, as discussed in [2]. For computer implementation, the modal expansions are truncated at M_i terms in the ith region. Equal numbers of TM^y and TE^y modes are retained so that the total number of modes in the ith region is $2M_i$. The field expansions are then matched at the $x = S/2$ and $x = W + S/2$ interfaces. The resulting homogeneous matrix equation yields the propagation constants when the determinant vanishes.

The number of modes retained in the expansions is constrained by the matrix equation and the edge condition. A square matrix requires that $2M_2 + 2M_3 = M_1 + M_4$. The edge condition requires that $M_2/M_1 = M_2/M_4 = c/d$ [4], which matches the spectral components along the interfaces. The accuracy of the solution is set by choosing the number of modes in one region.

After the homogeneous matrix equation is solved, the expansion coefficients in regions 1 and 4 are found by choosing one coefficient arbitrarily and then solving the resulting least squares problem using the QR factorization. The coefficients in regions 2 and 3 can then be easily computed.

As in [2], the problem is formulated entirely in real functions and only real solutions are searched for and computed. This limits the search to nonleaky solutions (of primary interest), but it greatly reduces the computation time.

The program was verified by computing the dispersion curve for a layered coupled-line microstrip. The results are shown in Fig. 3. The mode-matching results are compared with the results from a spectral-domain program. The spectral-domain results are for an open structure, while the mode-matching analysis includes the cover plate. The cover plate pushes β/β_0 higher by increasing the ratio of dielectric to air, with greater effect at lower frequen-

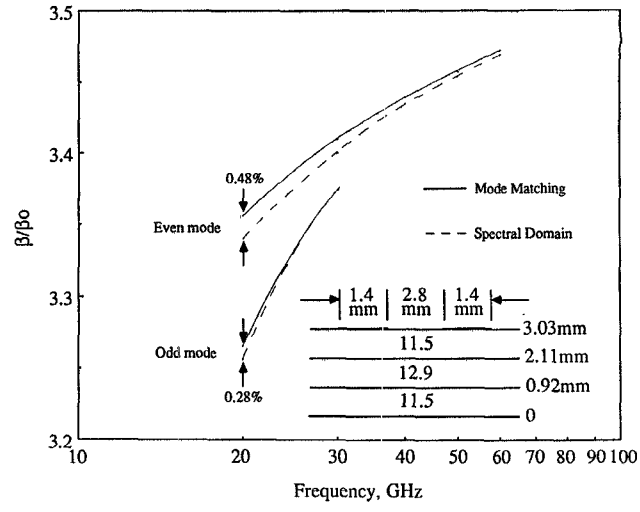

Fig. 3. Dispersion comparison for a layered microstrip. The spectral-domain results are for an open structure.

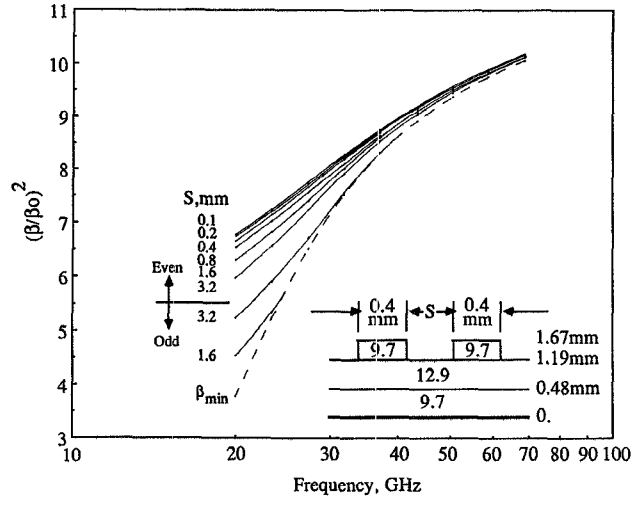

(a)

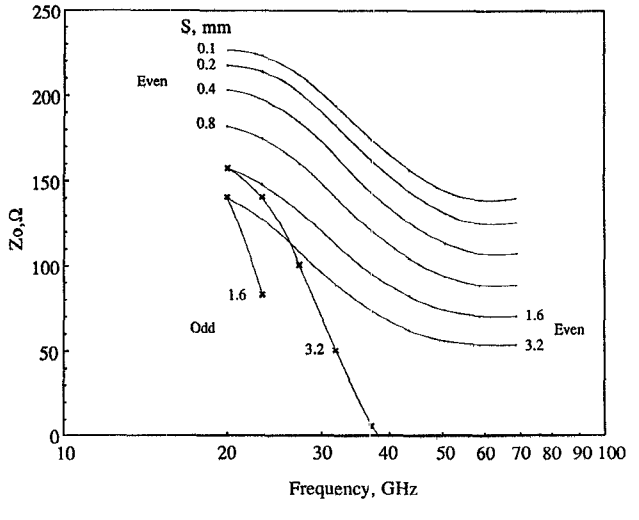

(b)

Fig. 4. Design charts for $\epsilon_1 = \epsilon_3 = 9.7$, $\epsilon_2 = 12.9$, $W = 0.4$ mm. (a) Dispersion. (b) Characteristic impedance.

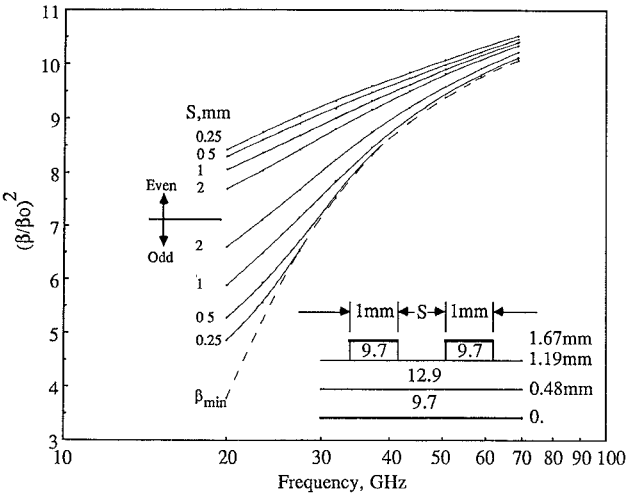

(a)

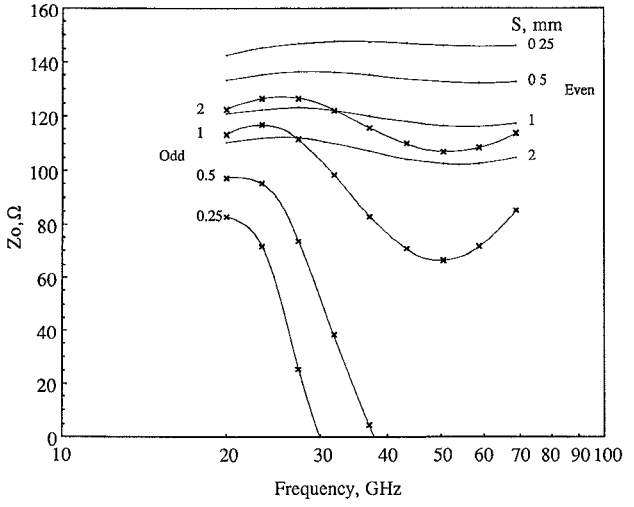

(b)

Fig 5. Design charts for $\epsilon_1 = \epsilon_3 = 9.7$, $\epsilon_2 = 12.9$, $W = 1$ mm. (a) Dispersion (b) Characteristic impedance.

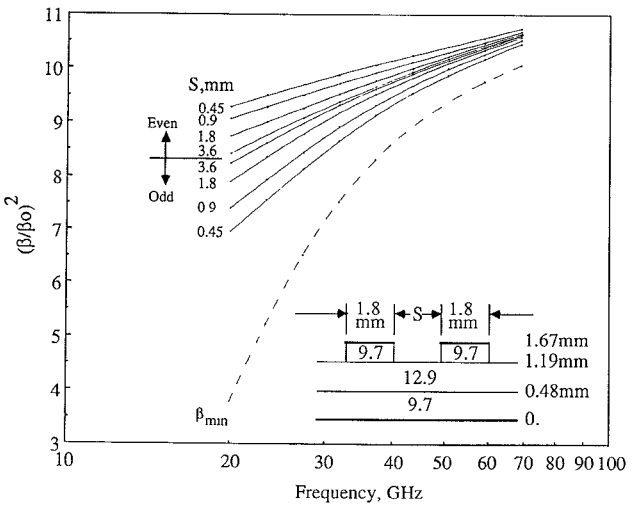

(a)

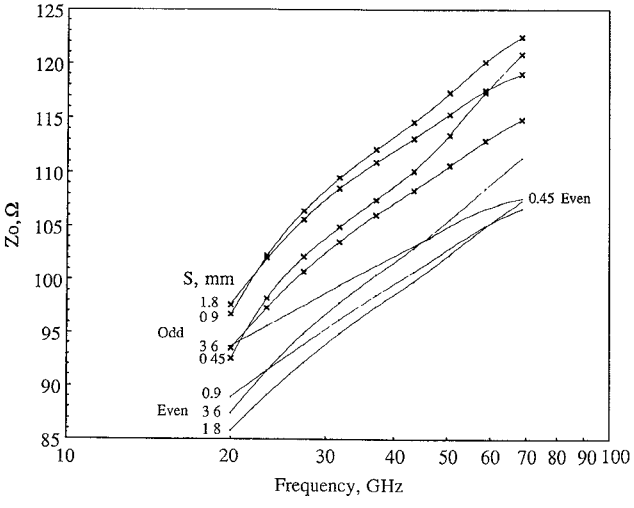

(b)

Fig. 6. Design charts for $\epsilon_1 = \epsilon_3 = 9.7$, $\epsilon_2 = 12.9$, $W = 1.8$ mm. (a) Dispersion. (b) Characteristic impedance.

cies, where the plate is electrically closer to the strips. Despite this, the agreement between the two results is excellent.

The power–voltage definition is used for the characteristic impedance for the reason given in [2]: poor behavior of the strip currents at high frequencies. Since a leaky mode has infinite power content, the characteristic impedance of a leaky mode is zero. This fact manifests itself as dips in the characteristic impedance design charts as modes become weakly bound.

III. Design Charts

The structure for which design charts are provided is the coupled-line version of the $\epsilon_1 = \epsilon_3 = 9.7$, $\epsilon_2 = 12.9$ single-line case from Fig. 11 in [2]. The coupled-line design charts corresponding to the $\epsilon_1 = \epsilon_3 = 8.2$, 11.5 single-line cases from Figs. 10 and 12 in [2] are not included due to the lack of space.

The coupled-line design charts with $\epsilon_1 = \epsilon_3 = 9.7$, $\epsilon_2 = 12.9$ for three different strip widths are given in Figs. 4–6. The dimensions are shown in the inset of the dispersion curves. The cover plate was set at the same height for which the single-line design chart in [2] was constructed to maintain consistency in the results. The coupled-line charts plot only the lowest order even and odd modes in their nonleaky regions. Modes below the dashed curves in the propagation constant charts are leaky and hence unsolvable by the techniques used here. Each design chart data point calculation for both the propagation constant and the characteristic impedance required on the order of 20–30 seconds on a Cray X-MP computer. Experimental verification of the charts is still required.

The convergence of the design chart pair (dispersion and impedance) for each strip width was tested at the extremes: low and high frequency, and small and large strip separation. Therefore, for each pair there are eight convergence plots, so they are omitted to save space. Generally, absolute convergence cannot be shown due to numerical instabilities and the excessive CPU time required. However, the convergent values can be estimated due to the semioscillatory behavior of the convergence curves, as demonstrated in [2]. We estimate the convergent values and place error brackets of ± 0.5 percent on the propagation constant and ± 1.5 percent on the characteristic impedance. The least number of modes required for all curves on all eight convergence plots to fall within the error brackets is used to calculate all data for the design chart. The numbers of modes used are $M_2 = 9$ for Fig. 4 and $M_2 = 8$ for Figs. 5 and 6.

The most restrictive convergence plot is usually the one for the propagation constant of the narrowest strip spacing at the lowest frequency. This is due to the field having least space in terms of wavelength to adjust to the structure. However, when the odd mode is weakly bound at high frequencies, a small change in the propagation constant changes the decay rate away from the strips dramatically. This greatly affects the power contained in the mode and hence the characteristic impedance. In this case the odd-mode impedance at high frequencies sets the number of modes required. Generally, there exists a relation between the number of modes and the $\epsilon_2/\epsilon_1 = \epsilon_2/\epsilon_3$ dielectric step. Larger steps require more modes since the field has a more complicated structure in which to conform.

Numerical instabilities occur in the determinant calculation for large matrices. A single-precision (64-bit word) Gaussian elimination routine with partial pivoting was found to be insufficient for some calculations. A double-precision (128-bit word) version was tried with surprisingly no improvement in stability. It was found that a single-precision Gaussian elimination routine with *full* pivoting dramatically improves the numerical stability. The full pivoting routine was found to slow the overall computation by a factor of approximately 2 over the partial pivoting routine.

IV. Conclusions

A mode-matching method is applied to the analysis of coupled-line Microslab waveguide. The method is appropriate for analysis only and generally requires a long-word-length computer due to the large matrices encountered. Numerical stability can be improved by using full pivoting for the Gaussian elimination routine. Design is facilitated by repeated analysis to generate design charts. Design charts are provided for GaAs/alumina Microslab implementations.

Acknowledgment

The authors wish to thank Y.-D. Lin for computing the spectral domain data.

References

[1] H. B. Sequeira and J. A. McClintock, "Microslab™—A novel planar waveguide for mm-wave frequencies," in *5th Benjamin Franklin Symp. Dig.* (Philadelphia, PA), May 4, 1985, pp. 67–69.

[2] B. Young and T. Itoh, "Analysis and design of Microslab waveguide," *IEEE Trans. Microwave Theory Tech.*, vol. MTT-35, pp. 850–857, Sept. 1987.

[3] R. Mittra, Y.-L. Hou, and V. Jamnejad, "Analysis of open dielectric waveguides using mode-matching technique and variational methods," *IEEE Trans. Microwave Theory Tech.*, vol. MTT-28, pp. 36–43, Jan. 1980.

[4] R. Mittra and S. W. Lee, *Analytic Techniques in the Theory of Guided Waves*. New York: Macmillan, 1971.

Tests of Microstrip Dispersion Formulas

H. A. ATWATER, SENIOR MEMBER, IEEE

***Abstract*—A set of published formulas for the frequency dependence of the microstrip effective relative dielectric constant $\epsilon_{re}(f)$ is tested relative to an assemblage of measured data values for this quantity chosen from the literature. The r.m.s. deviation of the predicted from the measured values ranged from 2.3 percent to 4.1 percent of the seven formulas for $\epsilon_{re}(f)$ tested. A formula due to Kirschning and Jansen [10] showed the lowest average deviation from measured values, although the differences between the predictions of their formula and others tested are of the order of the error limits of the comparison process. It is concluded that the results indicate the suitability of relatively simple analytical expressons for the computation for microstrip dispersion.**

Manuscript received August 10, 1987; revised September 12, 1987.
The author is with the Naval Postgraduate School, Monterey, CA 93943.
IEEE Log Number 8718360.

I. Introduction

The widespread use of microstrip transmission line for microwave circuit construction has created a need for accurate and practical computational algorithms for the values of microstrip line parameters. For this purpose, the microstrip line is modeled as an equivalent TEM system at the operating frequency. For this quasi-TEM model, a characteristic impedance Z_0 and an effective relative dielectric constant: $\epsilon_{re} = (c/v_p)^2$ are defined, where v_p/c is the velocity of the waves on microstrip line normalized to the free-space velocity of light. Because the wave fields exist in two dielectric media, namely the substrate dielectric material and the ambient air, hybrid modes propagate on microstrip line, and the wave velocity is frequency-dependent. A knowledge of the dispersive relative dielectric constant $\epsilon_{re}(f)$ is required for microstrip circuit design.

Although computer-aided design (CAD) programs are available with capability for generating microstrip line parameters, an extensive development has been made of closed-form expressions which allow rapid computation of the parameters without the necessity of setting up of a CAD file [1]–[3]. Veghte and Balanis have recently shown that the use of closed-form expressions for $\epsilon_{re}(f)$ within a computer program for the study of transient pulses on microstrip facilitated the calculation and saved computer time [4]. They reviewed the origin of several closed-form expressions appearing in the literature [5]–[9] and compared their respective predicted values for $\epsilon_{re}(f)$ over a wide frequency range. The expressions tested were shown to be in relatively close agreement to their predictions of dispersive behavior, but no comparison was made of these results with experimentally observed values of $\epsilon_{re}(f)$. In literature presentations of closed-form expressions for $\epsilon_{re}(f)$ [5]–[9], their predictions have typically been shown in comparison with a limited selection of experimental data points over a small range of substrate dielectric constants and microstrip line dimensions. It is the purpose of the present work to compare predicted values of $\epsilon_{re}(f)$ from several closed-form expressions with experimentally measured data chosen from a wide range of sources.

II. Closed-Form Expressions

The microstrip dispersion expressions tested are shown below in (1) to (6). The algebraic forms of these expressions as shown in (1) to (6) have been modified from the form of their original presentation to bring them into a similar formalism for comparison here. In these expressions, $\epsilon_{re}(0)$ is the zero-frequency, or quasi-static value of ϵ_{re}, ϵ_r is the substrate relative dielectric constant, h is substrate height, w is the microstrip line width, Z_0 its characteristic impedance, $\mu_0 = 4\pi/10^7$ henrys/meter, f is frequency, and c the velocity of light.

1) W. J. Getsinger [5]:

$$\epsilon_{re}(f) = \epsilon_{re}(0)\frac{1 + K_1 f_{ni}^2}{1 + G f_{ni}^2} \tag{1}$$